Atmos. Chem. Phys. Discuss., 14, 33045–33088, 2014
www.atmos-chem-phys-discuss.net/14/33045/2014/
doi:10.5194/acpd-14-33045-2014

Atmospheric Chemistry and Physics Discussions

Isotopic effects of nitrate photochemistry in snow: a field study at Dome C, Antarctica

T. A. Berhanu[1,*], J. Savarino[1,2], J. Erbland[1], W. C. Vicars[1,], S. Preunkert[1], J. F. Martins[3], and M. S. Johnson[4]**

[1]Universite Grenoble Alpes, LGGE, 38000 Grenoble, France
[2]CNRS, LGGE, 38000 Grenoble, France
[3]LTHE, UMR 5564, UJF-Grenoble 1/CNRS-INSU/G-INP, Grenoble, France
[4]Copenhagen Center for Atmospheric Research, Department of Chemistry, University of Copenhagen, Universitetsparken 5, 2100 Copenhagen, Denmark
[*]now at: Physics Institute, Climate and Environmental Physics, University of Bern, 3012 Bern, Switzerland
[**]now at: Technical Services Program, Air Pollution Control Division, Colorado Department of Public Health and Environment, Denver, CO, USA

Received: 5 November 2014 – Accepted: 12 November 2014 – Published: 23 December 2014

Correspondence to: J. Savarino (jsavarino@ujf-grenoble.fr)

Published by Copernicus Publications on behalf of the European Geosciences Union.

Abstract

Stable isotope ratios of nitrate preserved in deep ice cores are expected to provide unique and valuable information regarding paleo-atmospheric processes. However, due to the post-depositional loss of nitrate in snow, this information may be erased or significantly modified by physical or photochemical processes before preservation in ice. We have investigated the role of solar UV photolysis in the post-depositional modification of nitrate mass and stable isotope ratios at Dome C, Antarctica during the austral summer of 2011/12. Two 30 cm snow pits were filled with homogenized drifted snow from the vicinity of the base. One of these pits was covered with a plexiglass plate that transmits solar UV radiation, while the other was covered with a different plexiglass plate having a low UV transmittance. Samples were then collected from each pit at a 2–5 cm depth resolution and a 10 day frequency. At the end of the season, a comparable nitrate mass loss was observed in both pits for the top-level samples (0–7 cm). At deeper levels (7–30 cm), a significant nitrate mass loss (ca. 30 %) was observed in the UV-exposed pit relative to the control field. From the nitrate stable isotope ratios and concentration losses measured in the snow nitrate exposed to solar UV, we have derived average apparent isotopic fractionations ($^{15}\varepsilon$, $^{18}\varepsilon$ and ^{17}E) of -67.8 ± 12 ‰, 12.5 ± 6.7 ‰ and 2.2 ± 1.4 ‰ for δ^{15}N, δ^{18}O, and Δ^{17}O, respectively. These values are fairly stable throughout the season and are in close agreement with the apparent fractionations measured in natural snow at Dome C. Meanwhile, for the control samples in which solar UV was blocked, an apparent average $^{15}\varepsilon$ value of -12.0 ± 1.7 ‰ was derived. The difference in the apparent $^{15}\varepsilon$ values obtained for the two experimental fields strongly suggests that solar UV photolysis plays a dominant role in driving observed nitrate mass loss and resulting isotopic fractionation. We have also observed an insensitivity of $^{15}\varepsilon$ with depth in the snowpack under the given experimental setup. This is due to the uniform attenuation of incoming solar UV by snow, as $^{15}\varepsilon$ is strongly dependent on the shape of the incoming light flux. Together with earlier work, the results presented here represent a strong body of evidence that solar UV photolysis is

ACPD
14, 33045–33088, 2014

the most relevant post-depositional process modifying the mass and stable isotope ratios of snow nitrate at low accumulation sites where most deep ice cores are drilled. Nevertheless, modeling the loss of nitrate in snow is still required before a robust interpretation of ice core records can be provided.

1 Introduction

Nitrate (NO_3^-), end-product of the oxidation of atmospheric nitrogen oxides (NO_x = $NO + NO_2$), is one of the most abundant ions present in polar ice and snow. Ice core nitrate mass and isotopic measurements have the potential to provide quantitative constraints on historic variations in atmospheric NO_x cycling and oxidative capacity (Mayewski and Legrand, 1990; Wolff, 1995). However, the interpretation of these paleo-records is problematic at sites with low snow accumulation rates, where post-depositional processes such as the desorption of nitrate species on snow grain, sublimation/condensation of water vapor and photolysis of nitrate have a major influence on the signal archived in firn and ice (Dibb et al., 1998; Honrath et al., 1999; Rothlisberger et al., 2002; Blunier et al., 2005; Frey et al., 2009; Wolff, 2013). While desorption is manifested by the physical release of HNO_3 from the snow-pack, photolysis involves bond breaking in NO_3^- and emission of the photoproducts, such as NO_x, HONO and the hydroxyl radical (OH), which can alter the oxidative capacity of the overlying atmosphere (Chen et al., 2001; Crawford et al., 2001; Domine and Shepson, 2002; Grannas et al., 2007; Meusinger et al., 2014).

The stable isotope ratios of nitrate ($\delta^{18}O$, $\Delta^{17}O$ and $\delta^{15}N$) have been identified as useful metrics to constrain NO_x chemistry (Savarino et al., 2007, 2013; Morin et al., 2008; Hastings et al., 2009; Vicars et al., 2013) and the post-depositional processing of nitrate in snow (Blunier et al., 2005; Frey et al., 2009; Erbland et al., 2013). Stable isotope measurements are reported as isotopic enrichments (δ) relative to reference, where R represents the elemental $^{17}O/^{16}O$, $^{18}O/^{16}O$, or $^{15}N/^{14}N$ ratio in the sample or reference material. The reference used in for oxygen isotope analysis is Standard Mean

ACPD
14, 33045–33088, 2014

Oceanic Water (SMOW) and the reference for nitrogen is atmospheric N_2. For practical reasons, δ values are typically reported in per mill (‰), as variations in isotopic ratios for natural samples occur within a very narrow range.

In order to constrain post-depositional effects on the concentration and stable isotope ratios of nitrate, it is necessary to have knowledge of the isotopic fractionation values (expressed using $^{15}\varepsilon$, $^{18}\varepsilon$, ^{17}E, see Eq. (1) for definitions), which are unique for each post-depositional process. Blunier and co-workers analyzed two surface ice cores from Dome C, Antarctica and determined a nitrogen isotopic fractionation ($^{15}\varepsilon$) of (-54 ± 10) ‰ (Blunier et al., 2005). In an attempt to reproduce this field observation in the laboratory, an artificial snow was irradiated with UV light in the 200–900 nm wavelength range and a $^{15}\varepsilon$ value of (-11.7 ± 1.4) ‰ was determined. The authors concluded that post-depositional modification must therefore result primarily from sublimation of snow/desorption of nitric acid, with only a minor contribution from photolysis. However, it was later confirmed that the light source used in this laboratory study possessed a different spectral distribution compared to solar spectra encountered in the field, and this could have had a confounding effect on the interpretation of the results obtained (Frey et al., 2009). This effect was shown experimentally in a recent laboratory study (Berhanu et al., 2014; Meusinger et al., 2014) by irradiating natural snow from Dome C using different UV-filters to match field conditions. Accordingly, isotopic fractionations became less negative and approached zero when irradiated with short wavelength UV-light and vice-versa due to the different overlaps of nitrate isotopologue cross-sections with the incoming UV. The $^{15}\varepsilon$ value of (-47.9 ± 6.8) ‰ derived for the experiment conducted using a 320 nm filter (closer to Dome C solar irradiance conditions), was in good agreement with the field observations of (-50 ± 10) ‰ and (-71 ± 12) ‰ by Frey et al. (2009) at Dome C. A recent field study by Erbland and colleagues determined an average apparent $^{15}\varepsilon$ value of (-59 ± 10) ‰ for the East Antarctic Plateau (Erbland et al., 2013).

A theoretical framework has been developed by Frey and colleagues in order to determine isotopic fractionations associated with photolysis (Frey et al., 2009). The

ACPD
14, 33045–33088, 2014

authors used the Zero Point Energy-shift model (ΔZPE) (Yung and Miller, 1997), convoluted with solar spectrum measured during summer solstice at Dome C, and determined a $^{15}\varepsilon$ value of −48 ‰, consistent with their field observations. However, photolytic isotopic fractionations based solely on the ZPE-shift model can be affected by limitations of the model, such as ignoring the change in shape and intensity of the absorption cross-sections during isotopic substitutions (Schmidt et al., 2011). In a recent study, a semi-empirical model was developed that is based on the ZPE-shift model but addresses some of the limitations mentioned above (Berhanu et al., 2014). This model enabled better estimation of the absorption cross-sections of nitrate isotopologues, which can be interpolated to a temperature of interest, thus providing a better estimate for isotopic fractionations under field conditions.

The currently existing field studies (Blunier et al., 2005; Frey et al., 2009; Erbland et al., 2013) derived apparent isotopic fractionations (denoted $^{15}\varepsilon_{app}$, $^{18}\varepsilon_{app}$ and $^{17}E_{app}$), that incorporate not only the isotopic effects of photolysis but also other processes with the potential to induce isotopic fractionation (desorption, re-oxidation and surface deposition). In addition, the isotopic fractionations obtained in the existing field studies cover a wider range of $^{15}\varepsilon$ values (−40 to −74.3 ‰) (Erbland et al., 2013). Therefore, further experimental and modeling studies are required to constrain the effects of photolysis on stable isotope ratios of nitrate in snow and to advance the interpretation of these measurements in snow and ice.

We have performed a field study at Concordia (Dome C), Antarctica (75°06′ S and 123°19′ E) during the Antarctic summer of 2011/12. The effect of UV-photolysis on snow nitrate and its associated effects on nitrate's stable isotopic composition were investigated. We have employed an isolation technique to produce UV-exposed and UV-unexposed samples in order to understand the role of photolysis in the post-depositional processing of snow nitrate. To the best of our knowledge, this is the first field study that has employed an isolation strategy to constrain specifically nitrate mass loss and the isotopic fractionation induced by photolysis from solar UV radiation.

ACPD
14, 33045–33088, 2014

2 Methods

2.1 Experimental design

Wind-blown snow (i.e., drifted snow) was collected at Dome C on 02 December 2011 and physically homogenized in the field. This drifted snow possessed a high nitrate concentration (≈ 1600 ppb), which ensured levels adequate for isotopic analysis. Two snow pits of 1 m × 2 m surface area and 30 cm depth were excavated within close proximity (∼ 10 m) and filled with the drifted homogenized snow. A rectangular wooden frame was used to mark each surface level at a fixed position (i.e., depth = 0 cm). Hence, any additional windblown snow accumulating above this wooden mark could be removed on a weekly or as needed basis. The pits were covered with plexiglass plates of different UV transmittances (Fig. 1), one having only minor transmittance (10–15 %) below 380 nm, and the other allowing most of the solar UV-radiation in the 290–380 nm range. For simplicity, the samples exposed to UV will be referred to as "UV" samples, while those collected from the other pit, which is expected to be unaffected by UV-driven photolysis, will be referred to as "control" samples. Note that other non-UV light associated effects are expected to affect both pits equally (e.g., the disturbance of outgoing long-wave radiation caused by the plates). Equally, it should be realized that a complete protection from UV radiations in the field is impossible due to scattering of light by the snow, high solar zenithal angles (min at solstice 51.6°) and imperfection of the UV-cutting by the plexiglass. Such interferences are too complex to quantify but are mainly limited to the first cm of snow. The choice of the plexi-plates transmittance was based on the UV absorption cross-section of nitrate. Nitrate has UV absorption peaks around 200 and 305 nm, with the former being 3 orders of magnitude stronger than the latter (Mack and Bolton, 1999). However, light at the wavelengths of the strong 200 nm band is cut-off because of the presence of the stratospheric ozone layer (Fig. 2) and does not reach Earth's surface. The control plexi-plate blocks the secondary absorption band in contrast to the UV plexi-plates, which allow this band to reach the snow beneath. The plexiglass plates were placed on a metallic frame 20 cm above the snow

ACPD
14, 33045–33088, 2014

surface, which is expected to be an optimum height because it minimizes both the warming effect on the snow beneath and the trapping of emitted NO_x photoproducts. Placing the plates at a higher level could increase the possibility of snow deposition at the sides; furthermore, at higher solar zenith angles there may be solar UV radiation reaching the control plates. In contrast, vertical plates were not placed at the sides to avoid trapping drifted snow.

Sampling was conducted every 10 days from 2 December 2011 to 30 January 2012 at a 2–5 cm depth resolution and to a depth of 30 cm. Samples were collected less frequently at depths below the homogenized snow (i.e., down to 50 cm). The individual sampling events are indicated using numbers 0–6, with the numbers increasing from the beginning to the end of the season. Below 50 cm, the photolysis of nitrate becomes negligible, as demonstrated by the light transmission measured at Dome C (France et al., 2011). The detailed sampling dates are given in Table 1. For each sample, a snow mass of 0.5–1.0 kg was collected, placed into a two-liter (Whirl-Pack™) bag, and stored frozen. The samples were later melted at room temperature for nitrate concentration measurement and preconcentration. The concentration of nitrate in each sample was determined in a warm laboratory at the Dome C station using a continuous flow analysis method. This is a fast technique used in previous studies by our group at Dome C, with a precision of $< 3\,\%$ and a detection limit of $5\,\mathrm{ng\,g^{-1}}$ (Frey et al., 2009; Erbland et al., 2013). Most of the melted snow volume was preconcentrated using an anion exchange resin AG 1-X8 (Bio-Rad 200–400 mesh chloride form) to trap NO_3^- for isotopic analysis. This step is essential since some of the snow samples had initial nitrate concentrations of about $1.5\,\mathrm{nmol\,mL^{-1}}$, and a minimal amount of 100 nmol is required for stable isotopic analysis. The nitrate trapped in the resin was eluted with the addition of 5×2 mL 1 M NaCl solution (Frey et al., 2009; Erbland et al., 2013). The samples were stored in plastic tubes in the dark and shipped frozen to Grenoble, France for isotopic analysis. We have also collected surface snow samples along with the snow pit sampling in the immediate vicinity in order to observe if there is nitrate deposition

ACPD
14, 33045–33088, 2014

on the snow pits. The analysis of these samples was conducted in a similar fashion as for the snow pit samples.

2.2 Isotopic analysis

The oxygen and nitrogen isotopic composition of nitrate was determined using the bacterial denitrifier method (Sigman et al., 2001; Casciotti et al., 2002; Kaiser et al., 2007; Morin et al., 2008) as modified by Kaiser et al. (2007) and Morin et al. (2009). Briefly, a culture of the denitrifying bacteria (*Pseudomonas aureofaciens*) was concentrated 8 times by centrifugation following a 5–7 day growth period. 2 mL of the bacterial culture were then transferred to a 20 mL glass vial, which was sealed airtight with a PTFE septum. The vials were then degassed for 3 h using a helium flow (Air Liquide, 99.99 %). 100 nmol of each preconcentrated nitrate sample was then injected into these vials using an automated system (Gilson Liquid Handler 215). After an overnight incubation, which allows for complete conversion of NO_3^- to N_2O (Sigman et al., 2001), 0.5 mL of 1 M NaOH was added to each vial to inactivate the bacterial cells. The N_2O in the sample vial headspace was then flushed with purified helium (99.999 %) into a gold tube at 900 °C, where it was decomposed to O_2 and N_2 (Cliff and Thiemens, 1994; Kaiser et al., 2007), which were then separated by a GC column and passed to a MAT253 IRMS (Thermo Scientific) to determine the stable oxygen and nitrogen isotope ratios (Morin et al., 2009).

To correct for isotopic effects associated with sample analysis, we have included certified standards of USGS 32, USGS 34, and USGS 35 (Michalski et al., 2002; Bohlke et al., 2003), which were subjected to a treatment identical to the samples and prepared in the same matrix (1 M NaCl solution prepared using Dome C water in order to match the oxygen isotopic composition of local water) (Werner and Brand, 2001; Morin et al., 2009). A Python code was used to correct for blank effects and isotopic exchange, which can arise in cases of small sample size (provided in the Supplement). We have determined the overall accuracy of the method as the SD of the residuals derived from the linear regression between the measured and expected values of the reference

ACPD
14, 33045–33088, 2014

materials (Morin et al., 2009). For the samples analyzed in this study, the associated average uncertainties are 2.0, 0.4 and 0.6 ‰ for $\delta^{18}O$, $\Delta^{17}O$ and $\delta^{15}N$ respectively.

2.3 Data reduction

In order to quantify the effect of photolysis on the stable isotope ratios of snow nitrate, we have calculated apparent isotopic fractionations (isotopic fractionations derived for field samples irrespective of the process inducing fractionation) for O and N isotopes ($^{15}\varepsilon_{app}$, $^{18}\varepsilon_{app}$, and $^{17}E_{app}$ for $\delta^{15}N$, $\delta^{18}O$ and $\Delta^{17}O$ of nitrate, respectively) assuming an open system, where NO_x emitted upon the photolysis of nitrate will be removed as soon as it is formed and nitrate at depth is considered irreversibly lost (in contrast to the "skin layer" snow, which receives the deposition of re-oxidation products), and adopting the linear relation used in previous studies (Blunier et al., 2005; Erbland et al., 2013):

$$\ln(\delta + 1) = \varepsilon \ln(f) + \ln(\delta_0 + 1) \quad (1)$$

where f is the nitrate fraction remaining in snow, defined as the ratio of the final nitrate concentration (C) and the initial nitrate concentration (C_0) in the snow ($f = C/C_0$). δ_0 and δ are the isotope ratio values for the initial and final snow, respectively. C_0 was calculated using the average nitrate concentration measured at 25–30 cm depth, assuming there is no change in the amount of nitrate at this depth due to insufficient light penetration. The slope of the $\ln(\delta + 1)$ vs. $\ln(f)$ plot is the isotopic fractionation ε (note that $\varepsilon = (\alpha - 1)$, where α is the fractionation factor.

Isotopic fractionation due to photolysis (denoted $^{15}\varepsilon_{photo}$) has also been determined in this study using the Zero Point Energy shift-model (ΔZPE), as described in Frey et al. (2009). According to this model, during isotopic substitution, the ZPE of the heavier isotopologue is reduced, leading to a small blue shift in the absorption spectrum of the heavier isotopologue relative to the lighter one (Fig. 2). Hence, from a light isotopologue with a measured absorption cross-section ($^{14}NO_3^-$), it is possible to derive the absorption-cross section of the heavier isotopologue ($^{15}NO_3^-$) (Yung and Miller, 1997;

ACPD
14, 33045–33088, 2014

Miller, 2000). Isotopic fractionations (ε) were determined using the following equation:

$$\varepsilon = \frac{J'}{J} - 1 \tag{2}$$

where J' and J are the photolytic rate constants of the heavier and lighter isotopologues, respectively, defined mathematically as:

$$J = \int \Phi(\lambda,T)\sigma(\lambda,T)I(\lambda,\theta,z)\mathrm{d}\lambda \tag{3a}$$

$$J' = \int \Phi(\lambda,T)\sigma'(\lambda,T)I(\lambda,\theta,z)\mathrm{d}\lambda \tag{3b}$$

where σ and σ' are the absorption cross-sections of the light and heavy isotopologues respectively. $\Phi(\lambda)$ is the quantum yield and I is the actinic flux for the given wavelength ranges, these values are dependent on solar zenith angle (θ) and snow depth (z). Note that if $\Phi(\lambda)$ is assumed to be independent of wavelength and is the same both for $^{14}NO_3^-$ and $^{15}NO_3^-$, then there is no need to know its value in order to determine the isotopic fractionation value. In this study, we have applied this principle and derived isotopic fractionations for the UV-exposed pit in the presence of the plexi-plates and under field conditions.

We have also investigated the depth dependence of the isotopic fractionation values using the concentration and isotope ratio profiles of nitrate in natural (i.e., non-experimental) snow pits. Sampling at exactly the same depth during each collection was not possible under field conditions; therefore, the nitrate concentration and $\delta^{15}N$ values obtained for at least 4 different samples that were expected to be at the same depth, were used to derive the isotopic fractionation values. In a few cases, samples within a 1 cm depth differences were averaged together to derive $^{15}\varepsilon$.

ACPD
14, 33045–33088, 2014

2.4 Experimental precautions

It is important to present the experimental precautions taken in this study to minimize possible experimental artifacts. The two experimental fields were open to the atmosphere despite the presence of the plexi-plates. Therefore, while the deposition of snow/nitrate was prevented at the top of the experimental fields, drifted snow could still have been deposited at the surface of the pits, as the sides were not closed. In order to minimize this effect, we have a wooden frame at the sides of the snow pits so that it was possible to establish a reference surface level (depth = 0 cm), and the snow present above this frame was carefully removed as needed. In addition, in order to avoid absorption/reflection of solar UV by windblown snow deposited on top of the plexi-plates, we cleaned the plates at least 1–2 times per week. However, during strong winds and bad weather, it was impossible to keep the reference horizons always at the same level. The lack of homogeneity within and between fields is an unavoidable source of noise in the data obtained from this experiment.

3 Results

3.1 Concentration profiles

Figure 3 shows the fraction of nitrate remaining in the snow for each field and for each sampling event at 0, 2, 4 and 6×10 days (Plots for the nitrate fraction remaining in the snow with depth and the actual concentration for each sampling event are shown in Fig. S1 and Fig. S2). Accordingly, at the beginning of the experiment (UV #0 and control #0, $t = 0$), the concentration of nitrate was uniform with depth ($f \approx 1$). This corresponds to an average nitrate concentration of $(1431 \pm 46.8)\,\mathrm{ng\,g^{-1}}$ and (1478 ± 34.5) ng $\mathrm{g^{-1}}$ down to a 30 cm depth for the control and UV pits, respectively.

For control #2, f decreased to about 0.75 in the top 5 cm, but the profile stablized below 10 cm, with $f \approx 1$. A significant nitrate loss was observed for the controls #4 and

ACPD
14, 33045–33088, 2014

#6, with f reaching 0.15–0.25 in the top 4 cm, but with minor loss ($f > 0.8$) observed below 5 cm. The maximum nitrate loss ($f < 0.3$) was observed at the surface.

In contrast, samples from the pit exposed to UV radiation showed a significant decrease in nitrate mass up to a depth of 20 cm. For UV #2, a nitrate loss of $f \approx 0.5$ was observed at the surface. But at lower depths, below 3 cm, only minor loss was observed ($f > 0.8$). The maximum nitrate loss, with f reaching 0.2, was observed for UV #4 and UV #6. The loss continued until a depth of 7 cm where f reached 0.4. Further minor loss ($f > 0.75$) was observed up to a depth of 20 cm and the loss of nitrate ceased below 25 cm.

In general, the loss of nitrate in the top 7 cm was comparable for both the control and UV samples; however, the loss was larger for those samples exposed to solar UV relative to the control samples. Additionally, the amount of nitrate mass loss was different in each pit depending on depth and collection date.

For the surface snow samples, we have observed nitrate concentrations as high as 1500 ng g^{-1} in mid-December that decrease to 400 ng g^{-1} at the end of January (Fig. 4). This concentration profile sometimes matches the concentration of nitrate measured at a depth of 0–2 cm in the snow pits.

3.2 Isotopic analysis

Figure 5 shows the δ^{15}N profiles of the two pits for samples #0, #2, #4, and #6 (the δ^{15}N values for the duration of the sampling season are shown in Fig. S3). Controls #0 and #2 showed fairly uniform δ^{15}N, with values ranging between −10 and 0 ‰. However, controls #4 and control #6 exhibited enrichment in δ^{15}N up to +15 ‰ for the surface samples (0–2 cm depth) extending to a depth of about 7 cm and subtle changes below a 10 cm depth.

In the case of the UV samples, only UV #0 showed stability until a 30 cm depth, with δ^{15}N values ranging between −6 and −8 ‰. For the top 5 cm samples of UV #2, the δ^{15}N values showed an increasing pattern, with a maximum value at the surface (+12 ‰), and a stable δ^{15}N profile below 5 cm depth. Comparable δ^{15}N values and

ACPD
14, 33045–33088, 2014

similar profiles were observed for UV #4 and UV #6, with a maximum δ^{15}N value of +35 ‰ at a depth of 2–4 cm. However, a decrease in δ^{15}N values towards the surface level was observed, and this profile is not consistent for all samples. All of the UV samples (excluding UV #0, the $t = 0$ sample) have decreasing δ^{15}N values from their respective maximum value to about +8 to +14 ‰ near the snow surface (ca. 0–7 cm), irrespective of the sampling time. Meanwhile, this pattern is also apparent for the control #4 and control #6.

For the surface snow samples, δ^{15}N values varying between −10 and +40 ‰ were measured on different days (Fig. 6). However, no trend was observed in the δ^{15}N values over time. These values are sometimes similar to what is measured at the surface of the two pits.

Figure 7 shows the δ^{18}O values obtained for both the control and UV samples, which ranged from 52 to 68 ‰. It is difficult to detect a trend between δ^{18}O and depth or sampling period for either the control or UV samples in this data set.

Similar to the δ^{18}O observations, the measured Δ^{17}O values also exhibited no significant trend, with values ranging between 26 and 30 ‰ obtained for both pits (Fig. 8). However, comparing the control and UV samples, more variability is observed in the Δ^{17}O values of the UV samples.

In general, when comparing the stable oxygen isotope ratios of the control and UV samples, it is difficult to identify any pattern or significant difference between the two sets with respect to sampling event (Figs. 7 and 8). However, a significant difference is observed between the two pits (control and UV) for δ^{15}N. The measured δ^{15}N values are the main results used in this study to understand the role of photolysis in the post-depositional processing of snow nitrate.

3.3 Isotopic fractionations

Due to insignificant change in nitrate mass and isotopic composition, the linear fits for samples #0 and #1 from both pits were only weakly correlated, and are not discussed.

ACPD
14, 33045–33088, 2014

Robust correlations were observed for samples collected late in the season (a typical Rayleigh plot is shown in Fig. 9). The calculated nitrogen isotopic fractionation values (i.e., the slopes of the Rayleigh plots) for samples between 7 and 30 cm depth in the control and UV pits are collected in Table 2. The control samples had small negative isotopic fractionation values between (-7.4 ± 2.3) ‰ and (-15 ± 0.9) ‰. In contrast, the UV samples exhibited more highly negative nitrogen isotopic fractionations ranging from (-18.0 ± 7.3) ‰ to (-58.3 ± 20.0) ‰.

For the control pit samples, we have determined $^{18}\varepsilon$ values ranging from −2.1 to 3.9 ‰ and ^{17}E values of −1.4 to −0.8 ‰. However, the UV-exposed samples exhibited positive $^{18}\varepsilon$ values ranging 9.1 to 18.8 ‰ and ^{17}E values of 1.1 to 2.2 ‰.

3.4 Depth dependence of nitrogen isotopic fractionations

For the samples collected at a depth of 7–20 cm, the derived isotopic fractionations at each depth are shown in Fig. 10. We have calculated a nitrogen isotopic fractionation value ranging from −7.8 to −23.6 ‰ for the control samples in the 7–16 cm depth range. However, the UV samples exhibited more highly negative fractionations ranging from −52.2 to −65.9 ‰. The $^{18}\varepsilon$ and ^{17}E values derived with depth also have a very weak Rayleigh fitting at lower depth (below 10–15 cm), and are associated with large uncertainties. This is mainly due to the minor change in the oxygen isotopic signal, in contrast to the N isotopes, where relatively strong signals were obtained. Therefore, the $^{18}\varepsilon$ and ^{17}E data are not presented in this manuscript.

4 Discussion

4.1 Post-depositional isotopic effects

As this experimental study is built upon the comparison of two pits filled with drifted snow, our first priority was to ensure that the two pits were as identical as possible at the beginning of the study. Figures 3 and 5 show a uniform nitrate mass fraction left

ACPD
14, 33045–33088, 2014

in the snow ($f \approx 1$) as well as a fairly stable δ^{15}N (−6 to −8 ‰) profile up to a 30 cm depth for both UV #0 and control #0. This observation indicates that the snow was well homogenized and both pits had comparable initial nitrate concentration and isotopic composition.

However, a significant change was observed after consecutive sampling events. According to Figs. 3 and 5, loss of nitrate and enrichment in δ^{15}N was stronger in the UV pit than in the control pit. This phenomenon is also true at depth. These observations indicate that the presence of solar UV is fundamental in nitrate loss (Meusinger et al., 2014) and δ^{15}N enrichment (Berhanu et al., 2014), but it has a weaker effect on oxygen isotopes. However, even in the absence of direct solar UV light, a significant nitrate mass loss and isotopic fractionation was also observed in the top 0–7 cm of the control pit (grey shaded area in Fig. 3). This observation, together with the decreasing δ^{15}N pattern observed near the surface layers in opposition to the expected enrichment at similar depths, implies that additional processes besides photolysis such as wind deposition/removal of snow, desorption, or other unknown processes might be involved at this depth. Based on this theory, we have divided the two pits into two regions: the top 0–7 cm samples, where photolysis and additional processes are expected to act strongly, and samples collected at a 7–30 cm depth, where the effect of these additional processes is minor and photolysis is the dominant process inducing nitrate mass loss and isotopic fractionation. We have discussed below the possible causes for nitrate mass loss in the top 7 cm, which is summarized in Fig. 11.

Dome C generally experiences moderate wind speeds, with an average value of 2.9 m s^{-1} throughout the 1984–2003 meteorological record (Aristidi et al., 2005; Zhou et al., 2009), but even in this range of wind speeds deposition and removal of snow is possible at the surface. Even though the new snow deposited above the reference surface level was removed 1–2 times per week, the snow might have already been mixed with the underlying surface layer and manual removal may have disturbed or mixed the two layers, even with extremely careful handling. In addition, the drifted snow on the surface of the two pits was not always the same; more snow was often deposited

ACPD
14, 33045–33088, 2014

on one pit relative to the other, and the deposition was not homogeneous even within a single pit. This variability could have led to changes in the surface reference level between each sampling event and may have thus introduced additional artifacts in these samples.

Snowfall was not observed during the sampling period; therefore, direct deposition of nitrate via snowfall is discounted and, even if it were present, direct deposition will be negligible, as the tops of the snow pits were covered with the plexi-plates. An interesting observation was the convergence in both the nitrate concentration and δ^{15}N values near the surface. For the surface samples, both of these values converge on $f \approx 0.3$ and $\delta^{15}\mathrm{N} \approx +10$ to +14 ‰ (mainly in the UV #2–6 and control #4–6 samples). These values contradict expectations based on the concentration and δ^{15}N profile observed below 7 cm. This implies that there might be snow deposition or mixing at the surface of the pits with snow with a different isotopic composition ($\delta^{15}\mathrm{N} \approx +10$ to +14). As these measured values are sometimes in agreement with the surface snow measurements from a similar time period, the presence of deposition is inevitable. For example, on 10 January 2012 we observed drifted snow on both snow pits (refer to the field logbook in Supplement) with similar nitrate concentration and stable isotope ratios as the nearby surface snow measurement. However such events were sporadic and apparently depended on meteorological conditions.

Another important process to consider is the re-deposition of nitrate. NO_x photoproducts can be locally reoxidized to reform nitrate and become re-deposited on the snow surface, as the plexi-plate may have hindered the NO_x from escaping to the overlying atmosphere.

It should also be noted that desorption may have taken place from the surface of both of the pits, which could be enhanced by the plexi-plates trapping heat and warming the top layers. This effect should be manifested in both pits and should affect mainly the top few cm of the snow. The pits exhibited comparable loss of nitrate mass in the top 7 cm, but the δ^{15}N values were significantly different for the two pits, with minimum δ^{15}N values of −15.0 and −36.0 ‰ for the control and UV pit samples, respectively.

ACPD
14, 33045–33088, 2014

However, the more highly negative isotopic fractionation observed for the UV samples was probably due to the dominance of photolysis over the non-photolytic processes present in both pits.

Another possible reason for the observed nitrate mass loss and resulting isotopic effect could be photolysis in both pits. The plexi-plate over the control pit excluded the majority of UV light below 380 nm. However, 10–20 % of the incoming solar UV up to a wavelength range of ca. 310 nm is transmitted through this plate (Fig. 1), thus resulting in a spectral distribution in the control pit that overlaps with the nitrate UV absorption band. Additionally, at higher solar zenith angles, there might be direct solar UV impeding upon the sides of the plexi-plates leading to photolysis.

In general, there are multiple processes (Fig. 11) that can alter the concentration and isotopic composition of nitrate in the top 7 cm of snow. Identifying these processes and quantifying them is beyond the scope of this study. Hence, the samples from 7–30 cm depth range will be mainly considered in this manuscript.

4.1.1 The Nitrogen isotopic fractions: $^{15}\varepsilon$

Figure 12 shows the $^{15}\varepsilon$ values determined for the control and UV samples collected below 7 cm. The control samples possessed nearly constant $^{15}\varepsilon$ profiles whereas the isotopic fractionation values for the UV samples became progressively more negative over time. According to this figure, it seems that either $^{15}\varepsilon$ evolves over time (i.e., from collection event #2 to #6) or there is an artifact introduced by removing the samples collected in the top 7 cm, where relatively larger nitrate mass loss and isotopic fractionation was observed. The bending pattern in δ^{15}N observed for samples near the surface layers implies either the presence of another process or contamination by wind-blown snow with a different isotopic composition, as discussed in Sect. 4.1; therefore, we have excluded the samples from the surface level to where the δ^{15}N begins to shift to more negative values, and then recalculated the isotopic fractionations. Note that as drifted snow was not homogeneous within a given pit, the sampling may not have been performed evenly over time. The plots made based on these corrections are shown in

ACPD
14, 33045–33088, 2014

Fig. 12. Accordingly, $^{15}\varepsilon$ values ranging between −59.8 and −73.0 ‰ were obtained, irrespective of the sampling time. Therefore, the pattern observed under the first assumption (i.e., excluding all points in the top 7 cm) introduced an apparent evolution of $^{15}\varepsilon$ over time as an artifact of the analysis. The average apparent isotopic fractionation values derived using the second approach (−67.8 ± 12 ‰) are in excellent agreement with previous average apparent isotopic fractionations of −60 ± 10 ‰ at Dome C (Frey et al., 2009) and −59 ± 10 ‰ for the East Antarctic Plateau (Erbland et al., 2013) (Table 3).

Based on the significant difference between the $^{15}\varepsilon$ values of the control and UV samples, it is clear that the more highly negative isotopic fractionation is associated with solar UV photolysis. However, the small negative nitrogen isotopic fractionation (an average of −12.3 ± 1.7 ‰) observed for the control samples may be due to a combination of sublimation/desorption and minor photolysis. Even if a comparable mass loss of nitrate was observed in the top 7 cm of both pits, the δ^{15}N values are significantly different (Fig. 5). As the absorption cross section of nitrate is limited below 340 nm, photodissociation of nitrate is not expected to take place above 375 nm (i.e., the cut-off of the control plexi-plate). However, minor contributions from the average 15 % transmittance of the control plexi-plate and/or direct solar UV photolysis at high solar zenith angles and UV light scattering by the snow could potentially have resulted in some minor photolysis in the control pit, even if no systematic bias was observed between edge and center samples. This implies that another process (e.g., sublimation of snow, desorption of nitrate) could possibly take place and produce significant nitrate loss with only a minor change in isotopic composition. In a recent study of post-depositional isotopic effects in snow nitrate, it was verified that sublimation of snow leads to an overall ^{15}N isotopic fractionation close to zero (0.9 ± 1.5 ‰ at −30 °C, a temperature relevant at Dome C), whereas photolysis induces a highly negative fractionation ($^{15}\varepsilon$ = −59 ± 10 ‰) (Erbland et al., 2013). Therefore, a mixing of the evaporative and photolytic fractionation processes could conceivably result in an isotopic fractionation on the order −12 ‰ in the control pit. In contrast, photolysis is the dominant process in the UV pit due to the presence of

ACPD
14, 33045–33088, 2014

unobstructed solar UV, and we have determined highly negative isotopic fractionations ($^{15}\varepsilon = -67.8 \pm 12.0$ ‰). Considering the presence of multiple processes and the difficulty of isolating only photolysis under field conditions, we cannot consider the values derived from the UV pits to represent purely photolytic isotopic fractionation values, but rather apparent $^{15}\varepsilon$ values, impacted minimally by non-photolytic processes. In a recent laboratory study by Berhanu et al. (2014), who irradiated natural snow collected at Dome C using a UV lamp with a 320 nm filter (similar to field conditions), a $^{15}\varepsilon_{photo}$ of -47.9 ± 6.8 ‰ was reported (Berhanu et al., 2014). The less negative $^{15}\varepsilon$ value obtained in this study may be the result of an inability to fully reproduce the solar spectrum under laboratory conditions, in contrast to the field where the snow was exposed to natural solar UV.

We have also made a comparison between the isotopic fractionations obtained from the field study and a theoretical estimate made using the ΔZPE-shift model, as described in Frey et al. (2009) and recently modified by Berhanu et al. (2014). The newly modified model incorporates changes in width and amplitude, in addition to changes in the center wavelength, during isotopic substitution. By applying a 1 % width reduction factor and an amplitude increase of 1 %, in addition to a shift of $-32.5\,cm^{-1}$ in the center of the absorption cross section of $^{14}NO_3$ when substituted by $^{15}NO_3$, the authors derived an apparent $^{15}\varepsilon$ value of −55.1 ‰ under Dome C conditions (Berhanu et al., 2014). Following this approach and considering the solar UV transmittance of the plexiplates, as well as using the solar actinic flux measured at Dome C on 7 January 2012 at 2 p.m. local time (G. Picard, personal communication, 2013), we have calculated a $^{15}\varepsilon_{photo}$ value of −52.6 ‰ for the UV exposed pit. This value is also in agreement with the $^{15}\varepsilon_{photo}$ obtained from the laboratory study, but higher than the value determined for the UV pit, implying complications arising from multiple processes in the field study.

In general, even though we attempted to reduce the non-photolytic processes as much as we could, the observations cannot be considered as being derived from a purely photolytic isotopic fractionation in the field. However, the $^{15}\varepsilon$ values obtained

ACPD
14, 33045–33088, 2014

here (−67.8 ± 12.0 ‰) can be used as an apparent isotopic fractionation for Dome C where external non-photolytic processes are minimized as much as possible.

4.1.2 Oxygen isotopic fractionations: $\delta^{18}O$ and $\Delta^{17}O$

The control samples have $^{18}\varepsilon$ values close to zero (an average value of 0.2 ± 2.6 ‰) due to an insignificant change in isotopic values (Fig. 13). In contrary, except for sample UV #3, which exhibited a slightly higher $^{18}\varepsilon$ value (18.8 ± 5.5 ‰), the UV samples have nearly stable values ranging from 9.0–13.0 ‰ (an average value of 12.5 ± 6.7 ‰), in good agreement with previous measurements (Table 4).

The ^{17}E values for the control samples were not significantly different from zero, whereas the UV samples possessed an average ^{17}E value of (2.2 ± 1.4) ‰, in excellent agreement with previous studies (Table 4). This is probably due to the "cage effect", wherein the photoproducts resulting from the photolysis of nitrate immediately undergo isotopic exchange with the surrounding OH/water ($\Delta^{17}O \approx 0$) and reform secondary nitrate with $\Delta^{17}O$ values approaching zero (McCabe et al., 2005). However, compared to the variations observed in snow and ice below the photic zone (> 5 ‰) (Erbland et al., 2013; Sofen et al., 2014), changes of $\Delta^{17}O$ due to the cage effect (ca. 2 ‰) can be considered negligible. Another interesting observation is the greater scattering of the $\Delta^{17}O$ observed for the UV pit, clearly pointing the radiations as the source of this cage effect phenomena.

4.1.3 Depth dependence of isotopic fractionations

We have observed a stable nitrogen isotopic fractionation value with depth, and the average $^{15}\varepsilon$ value of (−59.9 ± 24.7) ‰ derived for samples collected between 7 and 30 cm is in good agreement with the average apparent isotopic fractionation of (−67.9 ± 12.0) ‰ derived from the experimental UV-exposed pit. The large error bars in Fig. 10 are due to the small sample size and the relatively large uncertainty in the depth measurement, as all the layers might not have been at exactly the same depth

ACPD
14, 33045–33088, 2014

during each sampling event, which may have led to the mixing of layers. The depth could have also changed over the course of the study due to the densification of the snow with time. The insensitivity of $^{15}\varepsilon$ with depth implies that, even if the number of photons decreases with depth in the snowpack, the shape of the solar actinic flux is not strongly altered, at least to the depth considered in this study. Berhanu et al. (2014) also observed similar depth insensitivity of the nitrogen isotopic fractionations in their laboratory study, where snow from Dome C was irradiated with a UV lamp closely matching the solar irradiance encountered at Dome C. From their measurement of actinic flux with depth in a snow column, a uniform attenuation of incoming flux was observed, leading to almost constant $^{15}\varepsilon$ values with depth in the snow column. The insensitivity of $^{15}\varepsilon$ with depth is a useful feature for the analysis of δ^{15}N records obtained from deep ice cores used to understand past atmospheric changes, simplifying the interpretation of the δ^{15}N records associated with solar UV-photolysis at different depths. Different modeling studies (such as the TRANSIT model (Erbland, 2011)) are currently attempting to use ice core $\delta^{15}\mathrm{N}(\mathrm{NO}_3^-)$ records to constrain historic variations in atmospheric oxidation capacity, changes in the ozone column, and solar variability. However, further detailed studies will be required to better constrain the obtained isotopic fractionations, especially for oxygen isotopes.

5 Conclusions

In this experimental study conducted at Dome C, we have investigated the effect of photolysis on the concentration and stable isotope ratios of nitrate in snow by comparing two identical snow pits, with one of the two exposed to solar UV. Using the combined concentration and δ^{15}N signals, we have determined an average $^{15}\varepsilon$ value of (-67.9 ± 12) ‰ for the UV-exposed samples collected at a 10 day frequency between 1 December 2011 and 30 January 2012. These values were fairly stable throughout the season and are in good agreement with previously determined isotopic fractionations at

ACPD
14, 33045–33088, 2014

Dome C. However, these values are significantly different from the $^{15}\varepsilon$ values obtained for the control samples (-12.3 ± 1.7 ‰).

When compared to the $^{15}\varepsilon$ values of (-47.9 ± 6.8) ‰ obtained in a laboratory experiment by Berhanu et al. (2014), where the photolytic process was isolated, the measured values for the UV-exposed samples are slightly lower (i.e., more highly negative). This difference might be associated with experimental design, as the laboratory conditions do not exactly replicate the solar spectrum, even if better control is possible in terms of temperature stability, and product removal relative to the field experiment. Other confounding factors may include differences in the chemical domain of nitrate (Meusinger et al., 2014), or changes due to the temperature dependence of the nitrate absorption cross-section It should also be noted that the field experiments show small influences due to non-photolytic processes such as desorption, deposition, and/or contamination by windblown snow. However, we recommend the derived average $^{15}\varepsilon$ value of (-67.9 ± 12) ‰ as being representative of photolytic isotopic fractionation of nitrate in snow.

We have also determined the depth dependence of the isotopic fractionations from natural (i.e., non-experimental) snow pits and observed that the $^{15}\varepsilon$ values are nearly insensitive to depth. Despite the fact that the $^{15}\varepsilon$ values derived at different depths are associated with larger error bars, the observations are in good agreement with the laboratory study of Berhanu et al. (2014). In addition, previous studies did not show a strong change in the actinic flux spectrum as the photic zone is short and attenuation does not change strongly with wavelength (Meusinger et al., 2014).

However, it is also important to reiterate some possible limitations of this experiment. Due to mechanical modification during the filling of the experimental pits with windblown snow, the snow used in this study did not possess identical physical properties (grain size, compactness, optical properties, etc.) compared to the natural snowpack. This may have resulted in a modification of light scattering within the snowpack. Additionally, the snow used in this study possessed a nitrate concentration more than an order of magnitude higher than what is normally measured in snow pits at Dome C, and

ACPD
14, 33045–33088, 2014

this may have impacted nitrate chemistry in the experimental snow pits. However, to the best of our knowledge, our study is the first to attempt a replication of field constraints (natural shape and size, natural concentration and exposure, as well as meteorological conditions). Finally, we have not included some of the data points in the top layers of both pits due to possible complications due to multiple processes (sublimation, desorption, contamination, etc.). During this analysis, we may have also introduced a small artifact in our $^{15}\varepsilon$ values, and this should be kept in mind when applying the values obtained in this study.

The results obtained here, together with results described previously in the literature (Frey et al., 2009; Erbland et al., 2013; Berhanu et al., 2014) represent a strong body of evidence that solar UV photolysis is the most relevant post-depositional process modifying the mass and stable isotope ratios of snow nitrate at low accumulation sites, where most deep ice cores are drilled.

The Supplement related to this article is available online at doi:10.5194/acpd-14-33045-2014-supplement.

Acknowledgements. The research leading to these results has received funding from the European Community's Seventh Framework Programme (FP7/2007-2013) under the grant agreement number 237890. We would like to thank INSU for its financial support for lab experiments through its LEFE program. The Agence nationale de la recherche (ANR) is gratefully acknowledged for its financial support through the OPALE project (contract NT09-451281). The Institute Polaire Paul-Emile Victor (IPEV) supported the research and polar logistics through the program SUNITEDC No. 1011. This work has been partially supported by a grant from Labex OSUG@2020 (Investissements d'avenir – ANR10 LABX56. We would also like to thank Erwan Vince for his significant contribution in sample analysis.

ACPD
14, 33045–33088, 2014

References

Aristidi, E., Agabi, K., Azouit, M., Fossat, E., Vernin, J., Travouillon, T., Lawrence, J. S., Meyer, C., Storey, J. W. V., Halter, B., Roth, W. L., and Walden, V.: An analysis of temperatures and wind speeds above Dome C, Antarctica, Astron. Astrophys., 430, 739–746, doi:10.1051/0004-6361:20041876, 2005.

Berhanu, T. A., Meusinger, C., Erbland, J., Jost, R., Bhatthacharya, S. K., Johnson, M. S., and Savarino, J.: Laboratory study of nitrate photolysis in Antarctic snow, Part 2: Isotopic effects and wavelength dependence J. Chem. Phys., 140, 244306, doi:10.1063/1.4882899, 2014.

Blunier, T., Floch, G. L., Jacobi, H. W., and Quansah, E.: Isotopic view on nitrate loss in Antarctic surface snow, Geophys. Res. Lett., 32, L13501, doi:10.1029/2005gl023011, 2005.

Bohlke, J. K., Mroczkowski, S. J., and Coplen, T. B.: Oxygen isotopes in nitrate: new reference materials for $O^{18} : O^{17} : O^{16}$ measurements and observations on nitrate-water equilibration, Rapid Commun. Mass. Sp., 17, 1835–1846, doi:10.1002/Rcm.1123, 2003.

Casciotti, K. L., Sigman, D. M., Hastings, M. G., Bohlke, J. K., and Hilkert, A.: Measurement of the oxygen isotopic composition of nitrate in seawater and freshwater using the denitrifier method, Anal. Chem., 74, 4905–4912, doi:10.1021/Ac020113w, 2002.

Chen, G., Davis, D., Crawford, J., Nowak, J. B., Eisele, F., Mauldin, R. L., Tanner, D., Buhr, M., Shetter, R., Lefer, B., Arimoto, R., Hogan, A., and Blake, D.: An investigation of South Pole HO_x chemistry: comparison of model results with ISCAT observations, Geophys. Res. Lett., 28, 3633–3636, doi:10.1029/2001gl013158, 2001.

Cliff, S. S. and Thiemens, M. H.: High-precision isotopic determination of the $^{18}O/^{16}O$ and $^{17}O/^{16}O$ ratios in nitrous-oxide, Anal. Chem., 66, 2791–2793, doi:10.1021/Ac00089a031, 1994.

Crawford, J. H., Davis, D. D., Chen, G., Buhr, M., Oltmans, S., Weller, R., Mauldin, L., Eisele, F., Shetter, R., Lefer, B., Arimoto, R., and Hogan, A.: Evidence for photochemical production of ozone at the South Pole surface, Geophys. Res. Lett., 28, 3641–3644, doi:10.1029/2001gl013055, 2001.

Dibb, J. E., Talbot, R. W., Munger, J. W., Jacob, D. J., and Fan, S. M.: Air–snow exchange of HNO_3 and NO_y at Summit, Greenland, J. Geophys. Res.-Atmos., 103, 3475–3486, doi:10.1029/97jd03132, 1998.

Domine, F. and Shepson, P. B.: Air–snow interactions and atmospheric chemistry, Science, 297, 1506–1510, doi:10.1126/Science.1074610, 2002.

ACPD
14, 33045–33088, 2014

Erbland, J.: Isotopic constrains on the interpretation of the nitrate record in the Vostok ice core, Ph.D. thesis, Université Joseph Fourier – Grenoble I, Grenoble, France, 2011.
Erbland, J., Vicars, W. C., Savarino, J., Morin, S., Frey, M. M., Frosini, D., Vince, E., and Martins, J. M. F.: Air–snow transfer of nitrate on the East Antarctic Plateau – Part 1: Isotopic evidence for a photolytically driven dynamic equilibrium in summer, Atmos. Chem. Phys., 13, 6403–6419, doi:10.5194/acp-13-6403-2013, 2013.
France, J. L., King, M. D., Frey, M. M., Erbland, J., Picard, G., Preunkert, S., MacArthur, A., and Savarino, J.: Snow optical properties at Dome C (Concordia), Antarctica; implications for snow emissions and snow chemistry of reactive nitrogen, Atmos. Chem. Phys., 11, 9787–9801, doi:10.5194/acp-11-9787-2011, 2011.
Frey, M. M., Savarino, J., Morin, S., Erbland, J., and Martins, J. M. F.: Photolysis imprint in the nitrate stable isotope signal in snow and atmosphere of East Antarctica and implications for reactive nitrogen cycling, Atmos. Chem. Phys., 9, 8681–8696, doi:10.5194/acp-9-8681-2009, 2009.
Grannas, A. M., Jones, A. E., Dibb, J., Ammann, M., Anastasio, C., Beine, H. J., Bergin, M., Bottenheim, J., Boxe, C. S., Carver, G., Chen, G., Crawford, J. H., Dominé, F., Frey, M. M., Guzmán, M. I., Heard, D. E., Helmig, D., Hoffmann, M. R., Honrath, R. E., Huey, L. G., Hutterli, M., Jacobi, H. W., Klán, P., Lefer, B., McConnell, J., Plane, J., Sander, R., Savarino, J., Shepson, P. B., Simpson, W. R., Sodeau, J. R., von Glasow, R., Weller, R., Wolff, E. W., and Zhu, T.: An overview of snow photochemistry: evidence, mechanisms and impacts, Atmos. Chem. Phys., 7, 4329–4373, doi:10.5194/acp-7-4329-2007, 2007.
Hastings, M. G., Jarvis, J. C., and Steig, E. J.: Anthropogenic impacts on nitrogen isotopes of ice-core nitrate, Science, 324, 1288–1288, doi:10.1126/Science.1170510, 2009.
Honrath, R. E., Peterson, M. C., Guo, S., Dibb, J. E., Shepson, P. B., and Campbell, B.: Evidence of NO_x production within or upon ice particles in the Greenland snowpack, Geophys. Res. Lett., 26, 695–698, doi:10.1029/1999gl900077, 1999.
Kaiser, J., Hastings, M. G., Houlton, B. Z., Rockmann, T., and Sigman, D. M.: Triple oxygen isotope analysis of nitrate using the denitrifier method and thermal decomposition of N_2O, Anal. Chem., 79, 599–607, doi:10.1021/Ac061022s, 2007.
Mack, J. and Bolton, J. R.: Photochemistry of nitrite and nitrate in aqueous solution: a review, J. Photoch. Photobio. A, 128, 1–13, doi:10.1016/S1010-6030(99)00155-0, 1999.
Mayewski, P. A. and Legrand, M. R.: Recent increase in nitrate concentration of Antarctic snow, Nature, 346, 258–260, 1990.

ACPD
14, 33045–33088, 2014

McCabe, J. R., Boxe, C. S., Colussi, A. J., Hoffmann, M. R., and Thiemens, M. H.: Oxygen isotopic fractionation in the photochemistry of nitrate in water and ice, J. Geophys. Res.-Atmos., 110, D15310, doi:10.1029/2004jd005484, 2005.
Meusinger, C., Berhanu, T. A., Erbland, J., Savarino, J., and Johnson, M. S.: Laboratory study of nitrate photolysis in Antarctic snow. I. Observed quantum yield, domain of photolysis, and secondary chemistry, J. Chem. Phys., 140, 244305, doi:10.1063/1.4882898, 2014.
Michalski, G., Savarino, J., Bohlke, J. K., and Thiemens, M.: Determination of the total oxygen isotopic composition of nitrate and the calibration of a $\Delta^{17}O$ nitrate reference material, Anal. Chem., 74, 4989–4993, doi:10.1021/ac0256282, 2002.
Miller, C. E.: Photo-induced isotopic fractionation of stratospheric nitrous oxide, Abstr. Pap. Am. Chem. S., 219, U312–U312, 2000.
Morin, S., Savarino, J., Frey, M. M., Yan, N., Bekki, S., Bottenheim, J. W., and Martins, J. M. F.: Tracing the origin and fate of NO_x in the Arctic atmosphere using stable isotopes in nitrate, Science, 322, 730–732, doi:10.1126/Science.1161910, 2008.
Morin, S., Savarino, J., Frey, M. M., Domine, F., Jacobi, H. W., Kaleschke, L., and Martins, J. M. F.: Comprehensive isotopic composition of atmospheric nitrate in the Atlantic Ocean boundary layer from 65° S to 79° N, J. Geophys. Res.-Atmos., 114, D05303, doi:10.1029/2008jd010696, 2009.
Rothlisberger, R., Hutterli, M. A., Wolff, E. W., Mulvaney, R., Fischer, H., Bigler, M., Goto-Azuma, K., Hansson, M. E., Ruth, U., Siggaard-Andersen, M. L., and Steffensen, J. P.: Nitrate in Greenland and Antarctic ice cores: a detailed description of post-depositional processes, Ann. Glaciol., 35, 209–216, doi:10.3189/172756402781817220, 2002.
Savarino, J., Kaiser, J., Morin, S., Sigman, D. M., and Thiemens, M. H.: Nitrogen and oxygen isotopic constraints on the origin of atmospheric nitrate in coastal Antarctica, Atmos. Chem. Phys., 7, 1925–1945, doi:10.5194/acp-7-1925-2007, 2007.
Savarino, J., Morin, S., Erbland, J., Grannec, F., Patey, M. D., Vicars, W., Alexander, B., and Achterberg, E. P.: Isotopic composition of atmospheric nitrate in a tropical marine boundary layer, P. Natl. Acad. Sci. USA, 110, 17668–17673, doi:10.1073/pnas.1216639110, 2013.
Schmidt, J. A., Johnson, M. S., and Schinke, R.: Isotope effects in N_2O photolysis from first principles, Atmos. Chem. Phys., 11, 8965–8975, doi:10.5194/acp-11-8965-2011, 2011.
Sigman, D. M., Casciotti, K. L., Andreani, M., Barford, C., Galanter, M., and Bohlke, J. K.: A bacterial method for the nitrogen isotopic analysis of nitrate in seawater and freshwater, Anal. Chem., 73, 4145–4153, 2001.

ACPD
14, 33045–33088, 2014

Sofen, E. D., Alexander, B., Steig, E. J., Thiemens, M. H., Kunasek, S. A., Amos, H. M., Schauer, A. J., Hastings, M. G., Bautista, J., Jackson, T. L., Vogel, L. E., McConnell, J. R., Pasteris, D. R., and Saltzman, E. S.: WAIS Divide ice core suggests sustained changes in the atmospheric formation pathways of sulfate and nitrate since the 19th century in the extratropical Southern Hemisphere, Atmos. Chem. Phys., 14, 5749–5769, doi:10.5194/acp-14-5749-2014, 2014.

Vicars, W. C., Morin, S., Savarino, J., Wagner, N. L., Erbland, J., Vince, E., Martins, J. M. F., Lerner, B. M., Quinn, P. K., Coffman, D. J., Williams, E. J., and Brown, S. S.: Spatial and diurnal variability in reactive nitrogen oxide chemistry as reflected in the isotopic composition of atmospheric nitrate: results from the CalNex 2010 field study, J. Geophys. Res.-Atmos., 118, 10567–10588, doi:10.1002/Jgrd.50680, 2013.

Werner, R. A. and Brand, W. A.: Referencing strategies and techniques in stable isotope ratio analysis, Rapid Commun. Mass. Sp., 15, 501–519, doi:10.1002/Rcm.258, 2001.

Wolff, E.: Ice core studies of global biogeochemical cycles, chap. Nitrate in polar ice, 195–224, Springer-Verlag, New York, 1995.

Wolff, E. W.: Ice sheets and nitrogen, Philos. T. R. Soc. B, 368, 20130127, doi:10.1098/Rstb.2013.0127, 2013.

Yung, Y. L. and Miller, C. E.: Isotopic fractionation of stratospheric nitrous oxide, Science, 278, 1778–1780, doi:10.1126/Science.278.5344.1778, 1997.

Zhou, M. Y., Zhang, Z. H., Zhong, S. Y., Lenschow, D., Hsu, H. M., Sun, B., Gao, Z. Q., Li, S. M., Bian, X. D., and Yu, L. J.: Observations of near-surface wind and temperature structures and their variations with topography and latitude in East Antarctica, J. Geophys. Res.-Atmos., 114, D17115, doi:10.1029/2008jd011611, 2009.

ACPD
14, 33045–33088, 2014

Table 1. Sample ID's with their respective sampling dates during the Austral summer 2011/12 field campaign at Dome C, Antarctica.

Sample ID	Sampling date
UV#0 and control#0	01 Dec 2011
UV#1 and control#1	10 Dec 2011
UV#2 and control#2	21 Dec 2011
UV#3 and control#3	31 Dec 2011
UV#4 and control#4	10 Jan 2012
UV#5 and control#5	20 Jan 2012
UV#6 and control#6	30 Jan 2012

ACPD
14, 33045–33088, 2014

Table 2. The nitrogen isotopic fractionations determined for both pits excluding all the samples between 0–7 cm or using the δ^{15}N signal to identify if influenced by external processes.

Sampling No.	Removing all samples at 0–7 cm depth		Using the δ^{15}N signal to exclude some points in the UV-pit samples
	$^{15}\varepsilon_{control}$ $(\pm 1-\sigma)/‰$	$^{15}\varepsilon_{UV}$ $(\pm 1-\sigma)/‰$	$^{15}\varepsilon_{UV}$ $(\pm 1-\sigma)/‰$
2	-12.9 ± 1.9	-18.0 ± 7.3	-72.7 ± 9.7
3	-7.4 ± 2.3	-25.7 ± 13.8	-57.2 ± 27.9
4	-12.9 ± 2.4	-47.8 ± 10.0	-72.3 ± 12.9
5	-13.2 ± 1.1	-48.6 ± 18.9	-65.8 ± 5.0
6	-15.0 ± 0.9	-58.3 ± 20.0	-69.0 ± 11.8

ACPD
14, 33045–33088, 2014

Table 3. Apparent isotopic fractionations ($^{15}\varepsilon_{app}$) observed in previous studies compared to the results obtained here.

	$^{15}\varepsilon$/‰	Reference
$^{15}\varepsilon_{app}$/‰	−53.9 ± 9.7	Blunier et al. (2005)[a]
	−50.0 ± 10.0 (DC 04)	Frey et al. (2009)[a]
	−71.0 ± 12.0 (DC 09)	Frey et al. (2009)[a]
	−59.0 ± 10.0	Erbland et al. (2013)[b]
	−67.8 ± 12.0	This study[c]
$^{15}\varepsilon_{photo}$/‰	−48.0	Frey et al. (2009)[d]
	−47.9 ± 6.8	Berhanu et al. (2014)[e]

[a] Values determined for Dome C.
[b] An apparent average value derived for different locations on the East Antarctic Plateau.
[c] The $^{15}\varepsilon$ determined for the UV samples in this study.
[d] Determined using the ZPE shift model and using the solar actinic flux of Dome C derived from snow TUV model.
[e] A laboratory result observed using snow from Dome C and a Xe lamp with a UV-filter at 320 nm (relevant to Dome C conditions) (Berhanu et al. 2014).

ACPD
14, 33045–33088, 2014

Table 4. Compiled $^{18}\varepsilon$ and ^{17}E values obtained from this study for the UV samples and previous studies.

$^{18}\varepsilon_{UV}$ $(\pm 1-\sigma)/‰$	$^{17}E_{UV}$ $(\pm 1-\sigma)/‰$	Reference
6.0 ± 3.0 (DC 04)	1.0 ± 0.2	Frey et al. (2009)[a]
9.0 ± 2.0 (DC 09)	2.0 ± 0.6	Frey et al. (2009)[a]
8.7 ± 2.4	2.0 ± 1.0	Erbland et al. (2013)[b]
12.5 ± 6.7	2.2 ± 1.4	This study[c]

[a] Determined by Frey et al. (2009) at Dome C during the summer campaigns in 2004 and 2007.
[b] An average value determined by Erbland et al. (2013) for the Eastern Antarctic Plateau.
[c] An average value determined by this study for all the UV samples.

ACPD
14, 33045–33088, 2014

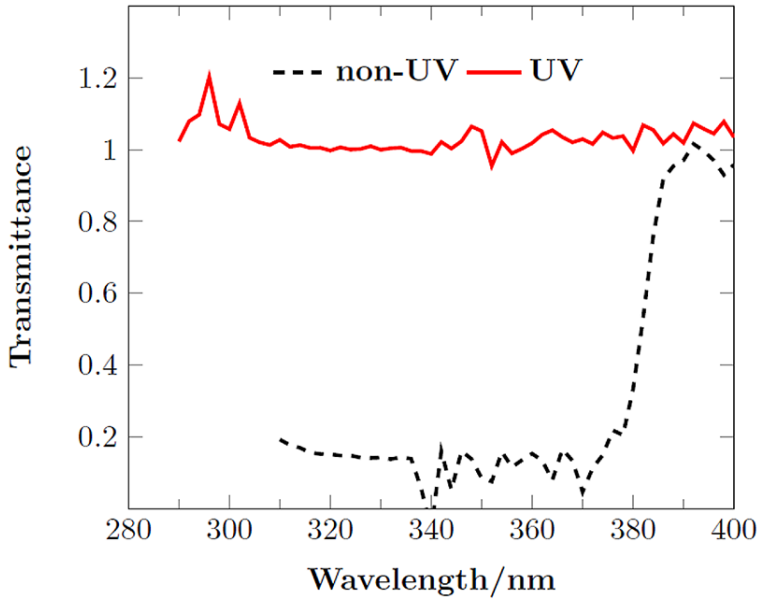

Figure 1. Transmittance as measured for the control and the UV plates. The UV plate transmits solar UV above 290 nm, whereas the control plate has a cut off at ca. 375 nm (note that the control plate has an average transmittance of 15 % below 375 nm).

ACPD
14, 33045–33088, 2014

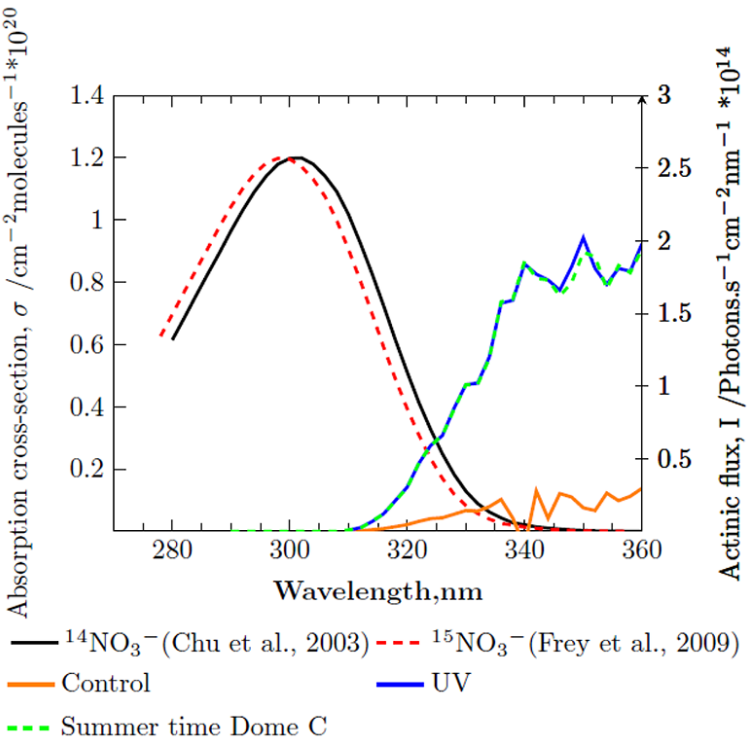

Figure 2. The absorption cross-section of $^{14}NO_3^-$ measured in the liquid phase and the absorption cross-section of $^{15}NO_3^-$ determined using the ZPE shift model (left *y* axis). The absorption cross section of $^{15}NO_3^-$ was derived by applying an average shift of 0.5 nm on $^{14}NO_3^-$. The 2 nm shift has been manually emphasized (note that in reality the two curves nearly overlap).Plotted on the right *y* axis is the solar spectrum derived using the TUV model at Dome C conditions (ozone column depth of 297 DU and an albedo of 0.9) and expected UV fluxes in the presence of the plexi-plate filters.

ACPD
14, 33045–33088, 2014

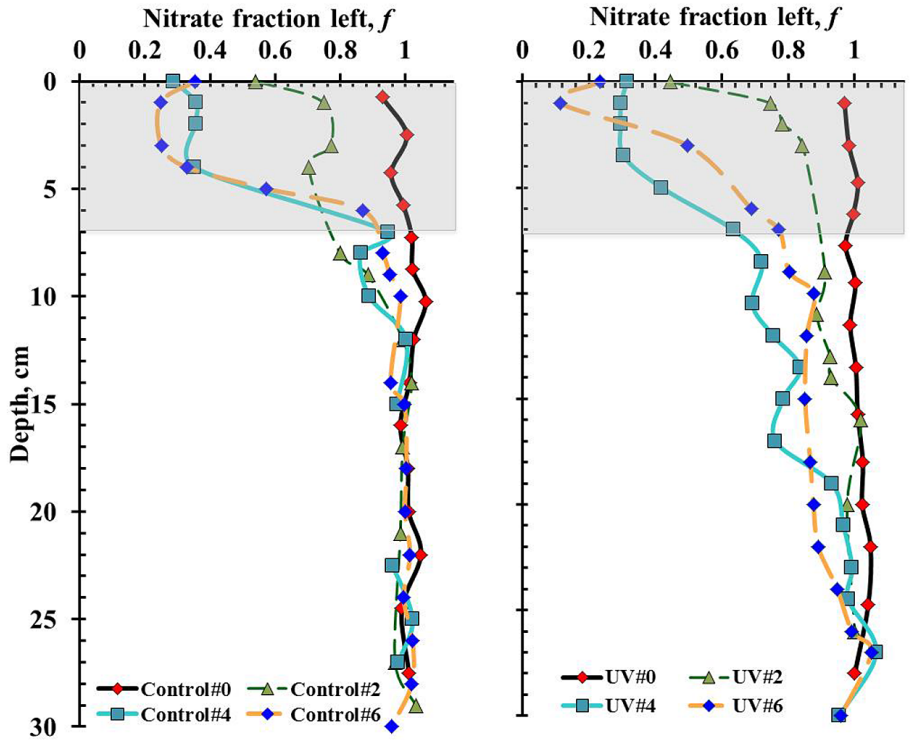

Figure 3. Plot of the nitrate fraction remaining in the snow (f) with depth. Control samples (unexposed to solar UV) are plotted in the left panel and UV-exposed samples are plotted in the right panel. The numbers denote the sampling events, which were carried out at 10 day intervals from 02 December 2011 to 30 January 2012. The grey shaded region shows the depth where external factors may play a significant role.

ACPD
14, 33045–33088, 2014

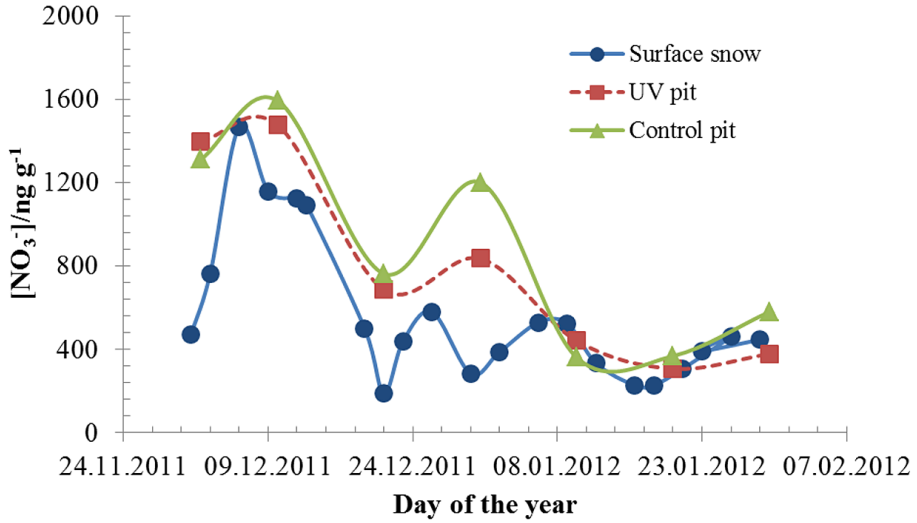

Figure 4. The nitrate concentration profile for the surface snow collected in the vicinity of the two pits compared with the UV and control pit surface snow (0–2 cm depth).

ACPD
14, 33045–33088, 2014

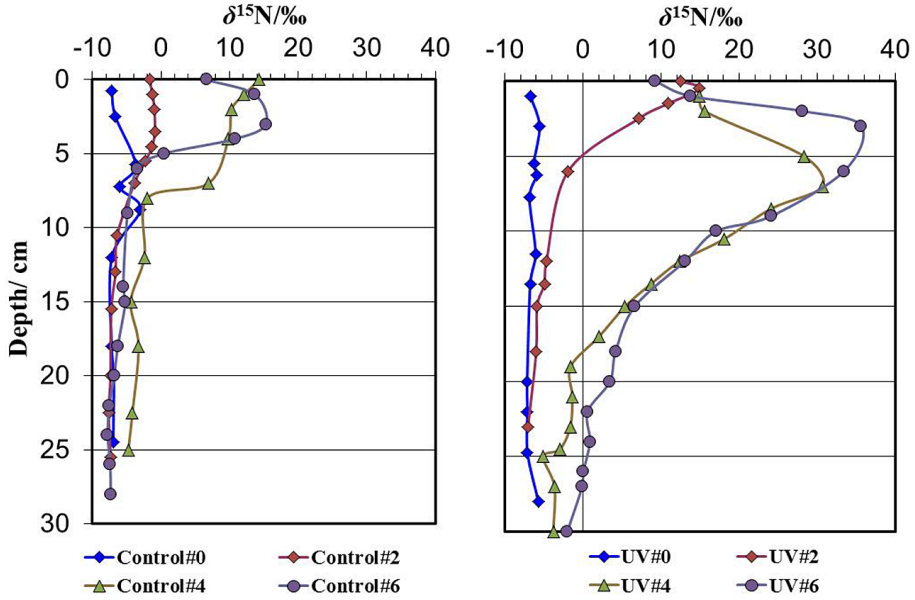

Figure 5. δ^{15}N depth profiles for snow nitrate in the control (top panel) and UV (bottom panel) pits.

ACPD
14, 33045–33088, 2014

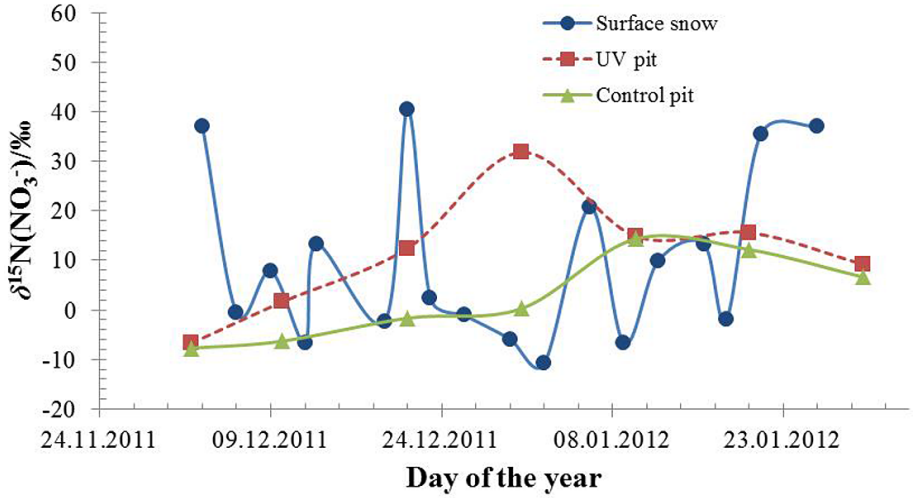

Figure 6. δ^{15}N time-series for nitrate in natural surface snow compared to surface snow sampled from the UV and control pits.

ACPD
14, 33045–33088, 2014

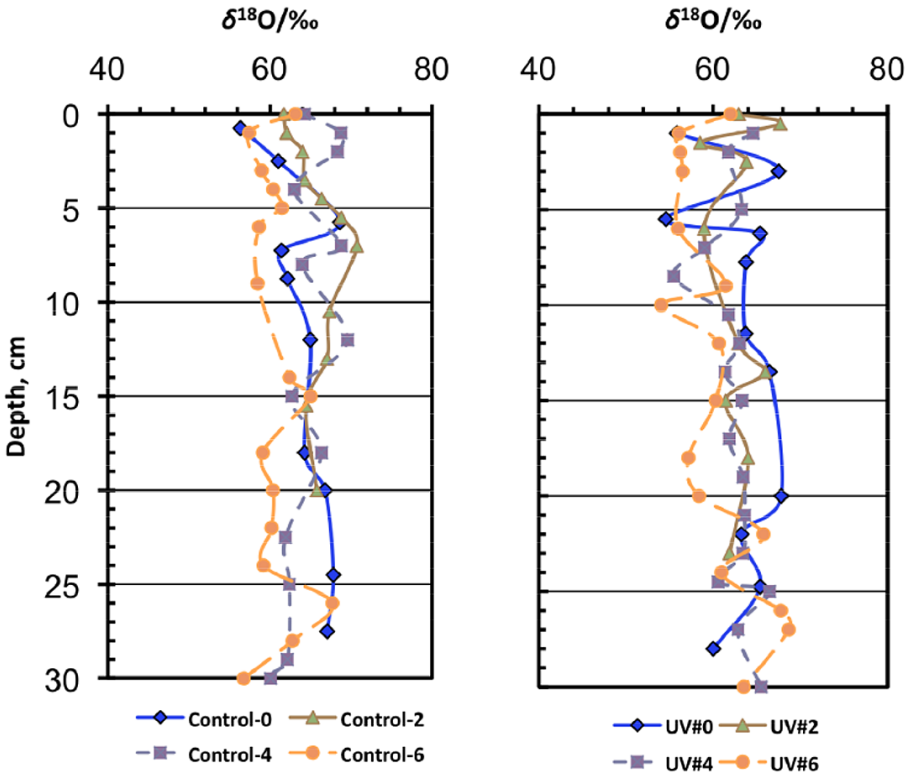

Figure 7. $\delta^{18}O$ depth profiles for snow nitrate in the control (left panel) and UV (right panel) pits.

ACPD
14, 33045–33088, 2014

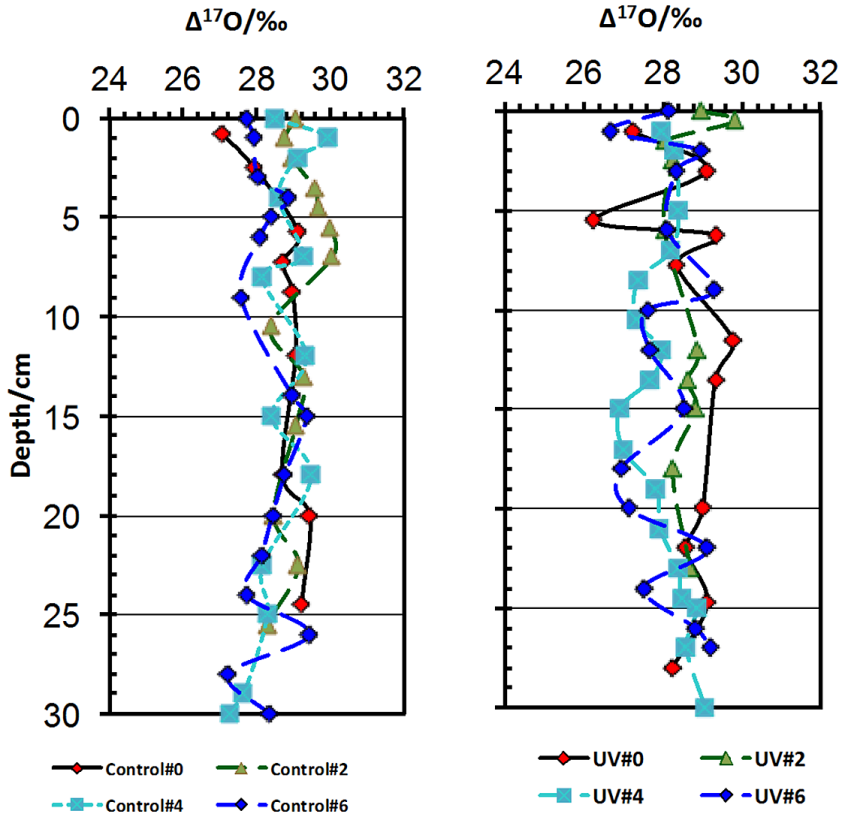

Figure 8. Same as Fig. 7 but for $\Delta^{17}O$.

ACPD
14, 33045–33088, 2014

Isotopic effects of nitrate photochemistry in snow

T. A. Berhanu et al.

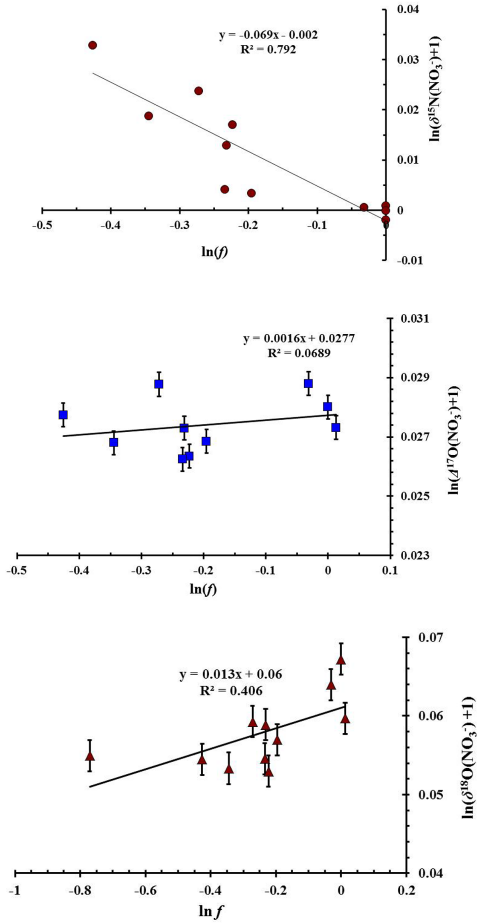

Figure 9. Rayleigh plots for the UV #6 samples. The error bars correspond to the analytical uncertainty of the isotopic measurements. Note that, the error bars are smaller than the size of the data points in the case of the Rayleigh plot for the δ^{15}N.

ACPD
14, 33045–33088, 2014

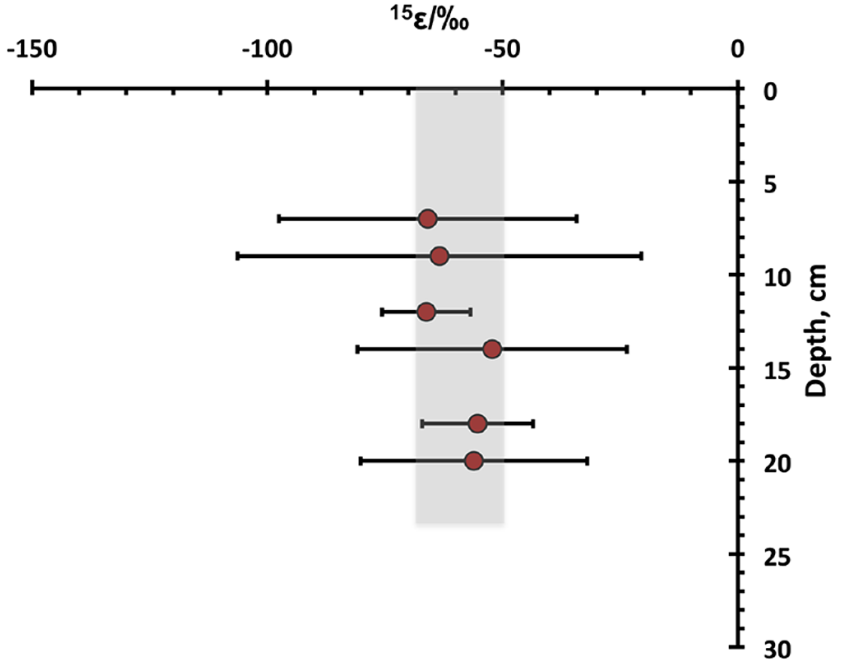

Figure 10. The depth profile of $^{15}\varepsilon$ for the UV pit. The $^{15}\varepsilon$ was calculated from samples collected at the same depth during each sampling event. Error bars are calculated using the least square fit method as in Frey et al. (2009). The shaded region represents the measured $^{15}\varepsilon$ range of −50 to −70 ‰.

ACPD
14, 33045–33088, 2014

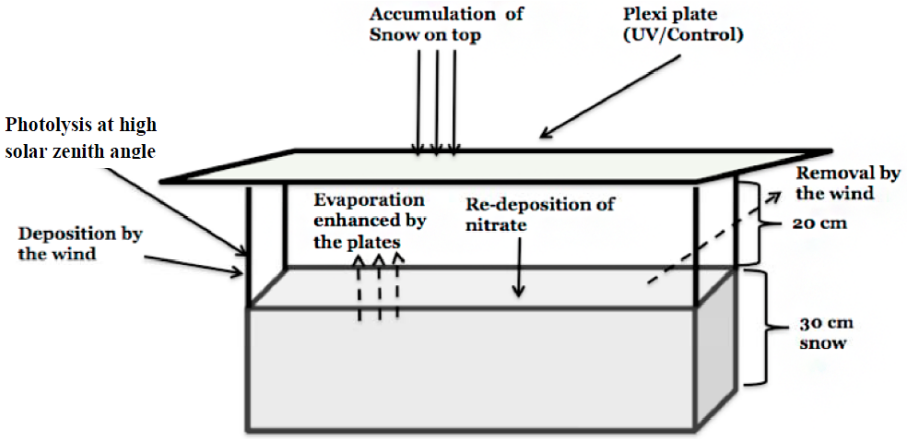

Figure 11. Schematic showing the possible external processes that could affect the surface layers of both the UV and control pits. These include evaporation, wind deposition/removal, and photolysis at high solar zenith angle.

ACPD
14, 33045–33088, 2014

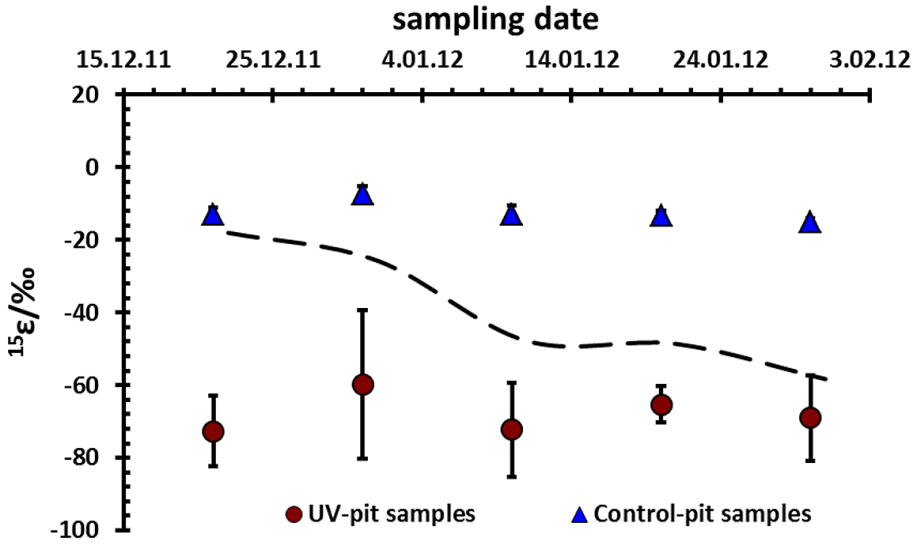

Figure 12. $^{15}\varepsilon$ values determined for the control samples (triangles), UV samples excluding all samples between 0–7 cm (dashed line), and the UV samples obtained using the δ^{15}N signal to identify data points affected by non-photolytic processes rather than by excluding all 0–7 cm data. Note that excluding the entire top 7 cm data introduced an apparent trend where $^{15}\varepsilon$ decreases with time. Errors are determined by the least square fit method as in Frey et al. (2009).

ACPD
14, 33045–33088, 2014

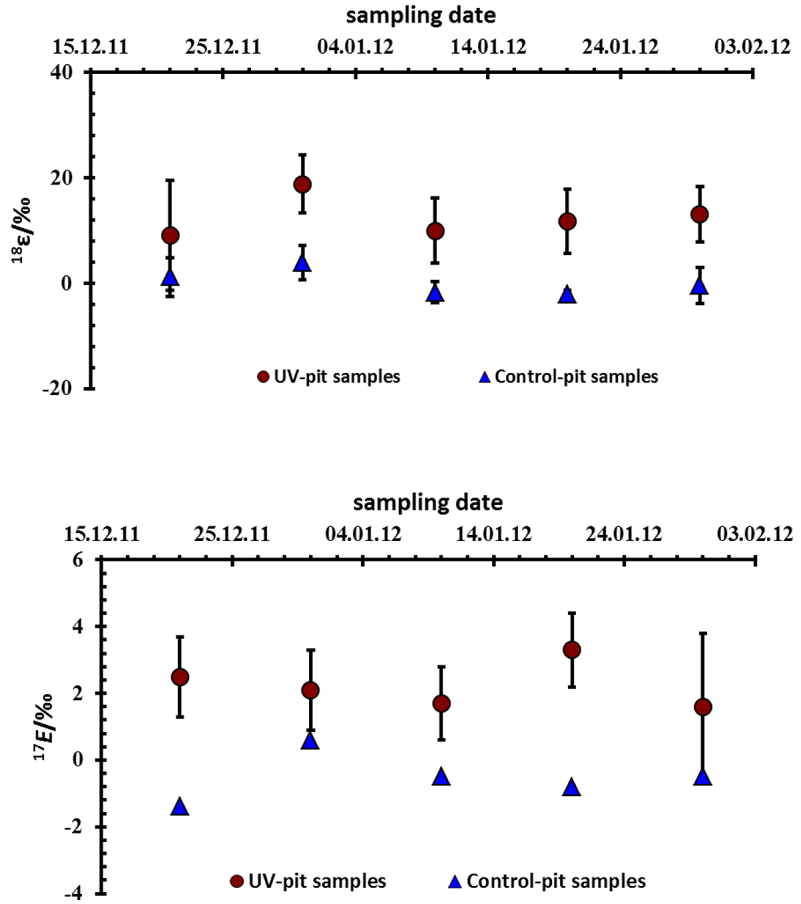

Figure 13. The $^{18}\varepsilon$ (top panel) and ^{17}E (bottom panel) values calculated for the two pits with respect to their sampling date. Errors are determined by the least square fit method from as in Frey et al. (2009).

ACPD
14, 33045–33088, 2014